Carbon Dioxide Capture for Storage in Deep Geologic Formations – Results from the CO_2 Capture Project

Capture and Separation of Carbon Dioxide from Combustion Sources

Edited by

David C. Thomas
Senior Technical Advisor
Advanced Resources International, Inc.
4603 Clearwater Lane
Naperville, IL, USA

Volume 1

ELSEVIER
2005

Amsterdam – Boston – Heidelberg – London – New York – Oxford
Paris – San Diego – San Francisco – Singapore – Sydney – Tokyo

Elsevier Internet Homepage – http://www.elsevier.com
Consult the Elsevier homepage for full catalogue information on all books, major reference works, journals, electronic products and services.

Elsevier Titles of Related Interest

AN END TO GLOBAL WARMING
L.O. Williams
ISBN: 0-08-044045-2, 2002

FUNDAMENTALS AND TECHNOLOGY OF COMBUSTION
F. El-Mahallawy, S. El-Din Habik
ISBN: 0-08-044106-8, 2002

GREENHOUSE GAS CONTROL TECHNOLOGIES: 6TH INTERNATIONAL CONFERENCE
John Gale, Yoichi Kaya
ISBN: 0-08-044276-5, 2003

MITIGATING CLIMATE CHANGE: FLEXIBILITY MECHANISMS
T. Jackson
ISBN: 0-08-044092-4, 2001

Related Journals:
Elsevier publishes a wide-ranging portfolio of high quality research journals, encompassing the energy policy, environmental, and renewable energy fields. A sample journal issue is available online by visiting the Elsevier web site (details at the top of this page). Leading titles include:

Energy Policy
Renewable Energy
Energy Conversion and Management
Biomass & Bioenergy
Environmental Science & Policy
Global and Planetary Change
Atmospheric Environment
Chemosphere – Global Change Science
Fuel, Combustion & Flame
Fuel Processing Technology

All journals are available online via ScienceDirect: www.sciencedirect.com

To Contact the Publisher
Elsevier welcomes enquiries concerning publishing proposals: books, journal special issues, conference proceedings, etc. All formats and media can be considered. Should you have a publishing proposal you wish to discuss, please contact, without obligation, the publisher responsible for Elsevier's Energy program:

Henri van Dorssen
Publisher
Elsevier Ltd
The Boulevard, Langford Lane
Kidlington, Oxford
OX5 1GB, UK

Phone: +44 1865 84 3682
Fax: +44 1865 84 3931
E.mail: h.dorssen@elsevier.com

General enquiries, including placing orders, should be directed to Elsevier's Regional Sales Offices – please access the Elsevier homepage for full contact details (homepage details at the top of this page).

ELSEVIER B.V.
Radarweg 29
P.O. Box 211, 1000 AE Amsterdam
The Netherlands

ELSEVIER Inc.
525 B Street, Suite 1900
San Diego, CA 92101-4495
USA

ELSEVIER Ltd
The Boulevard, Langford Lane
Kidlington, Oxford OX5 1GB
UK

ELSEVIER Ltd
84 Theobalds Road
London WC1X 8RR
UK

First edition 2005

Library of Congress Cataloging in Publication Data
A catalog record is available from the Library of Congress.

British Library Cataloguing in Publication Data
A catalogue record is available from the British Library.

ISBN: 0-08-044570-5 (2 volume set)

Volume 1: Chapters 8, 9, 13, 14, 16, 17, 18, 24 and 32 were written with support of the U.S. Department of Energy under Contract No. DE-FC26-01NT41145. The Government reserves for itself and others acting on its behalf a royalty-free, non-exclusive, irrevocable, worldwide license for Governmental purposes to publish, distribute, translate, duplicate, exhibit and perform these copyrighted papers. EU co-funded work appears in chapters 19, 20, 21, 22, 23, 33, 34, 35, 36 and 37. Norwegian Research Council (Klimatek) co-funded work appears in chapters 1, 5, 7, 10, 12, 15 and 32.

Volume 2: The Storage Preface, Storage Integrity Preface, Monitoring and Verification Preface, Risk Assessment Preface and Chapters 1, 4, 6, 8, 13, 17, 18, 19, 20, 21, 22, 23, 24, 25, 26, 27, 28, 29, 30, 31, 32, 33 were written with support of the U.S. Department of Energy under Contract No. DE-FC26-01NT41145. The Government reserves for itself and others acting on its behalf a royalty-free, non-exclusive, irrevocable, worldwide license for Governmental purposes to publish, distribute, translate, duplicate, exhibit and perform these copyrighted papers. Norwegian Research Council (Klimatek) co-funded work appears in chapters 9, 15 and 16.

♾ The paper used in this publication meets the requirements of ANSI/NISO Z39.48-1992 (Permanence of Paper).
Printed in The Netherlands.

Carbon Dioxide Capture for Storage in Deep Geologic Formations, Volume 1
D.C. Thomas and S.M. Benson (Eds.)

Chapter 9

SELF-ASSEMBLED NANOPOROUS MATERIALS FOR CO_2 CAPTURE PART 1: THEORETICAL CONSIDERATIONS

Ripudaman Malhotra[1], David L. Huestis[1], Marcy Berding[1], Srinivasan Krishanamurthy[1] and Abhoyjit Bhown[2]

[1]Physical Sciences Division, SRI International, Menlo Park, CA 94025, USA
[2]Bay Molecular Corporation, Newark, CA 94560, USA

ABSTRACT

Nanoporous materials have been shown to have very high adsorption capacities for gases. We examined their potential application in a PSA system to capture CO_2. Of particular interest to us was the range of self-assembled materials that could be generated from copper dicarboxylate systems. These salts have a square lattice whose cells could be tailored to accommodate multiple molecules of CO_2 and thereby optimize the material for maximum adsorption capacity. With multiple CO_2 molecules being adsorbed in each cell there is also the possibility that the system would display cooperative behavior. We describe here the thermodynamics of these systems and show that a significantly larger amount of an adsorbate species can be shifted between the vapor and adsorbed states for a given pressure swing. To further assess the potential benefits of using such materials, we simulated the breakthrough behavior of CO_2 from a packed bed containing activated carbon and copper terephthalate. These simulations show that for a given bed diameter, the appropriate bed length would be about a third that for carbon alone, even if copper terephthalate displayed no cooperativity. The bed length could be further reduced to a quarter if there were even a modest degree of cooperative binding.

INTRODUCTION

Concerns about CO_2 emissions and global warming are driving efforts to minimize CO_2 emissions. Power production, particularly from coal, is one of the major sources of CO_2. To sequester the CO_2, it is necessary to first concentrate it to a nearly pure form. This concentration can be achieved by using materials like lime or amines for absorbing CO_2 from the flue gas at a certain temperature (T_1) and then releasing it at a higher temperature (T_2). The problem with this scheme is that if the enthalpy of adsorption is high, T_2 must be high to release the CO_2. A higher T_2 means that valuable heat would be rejected, which would lead to reduced overall efficiency of the power plant. On the other hand, if the adsorption is not highly exothermic, the material is not very effective in absorbing CO_2 in the first place.

Inspired by the work of Seki [1–3] on copper dicarboxylate salts, we conducted research on nanoporous materials made of cells that would physisorb CO_2 by relatively weak van der Waals forces and that would be large enough to accommodate multiple CO_2 molecules. Seki et al., have shown these salts to have a very high capacity for adsorbing methane. Figure 1 shows one layer of copper oxalate, a representative of this family of framework solids. We anticipated that the CO_2 molecules would be held in the cavities (i.e. cells where CO_2 can bind). The dimensions of the square cavity can be tailored by the choice of the dicarboxylic acid.

We further conjectured that if the binding of CO_2 were cooperative, that is, if each subsequent molecule of CO_2 adsorbed in the cell had a slightly higher heat of adsorption, the adsorption isotherm would be steeper and it would require less work of a pressure swing to move an equivalent amount of CO_2 between the gas

and adsorbed phases. Examples of cooperative binding are known in enzyme-substrate systems [4], the binding of oxygen to hemoglobin being one commonly cited example of cooperative binding.

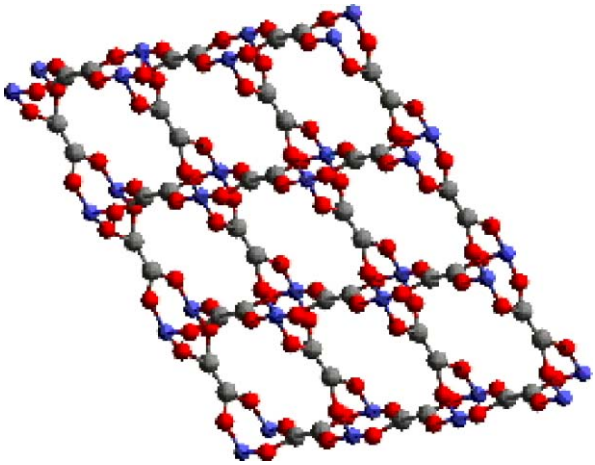

Figure 1: Simulated structure of copper oxalate.

The overall goal of this project was to design, synthesize, characterize, and test materials for capturing CO_2 in PSA systems. The project was conducted in two phases. In the first phase, lasting 9 months, the work focused on validating the concept of cooperative binding, determining the feasibility of copper dicarboxylate systems that could accommodate several CO_2 molecules in each pore, and estimating the potential benefits of using such material in a PSA system. The work conducted during this phase is described in this chapter. The accompanying chapter describes results from our experimental studies that were conducted in a subsequent phase, also lasting 9 months.

Thermodynamic Analysis

Optimal heat of adsorption

The optimal heat of adsorption (ΔH) can be determined by considering the free energy (ΔG) of the absorption and desorption of CO_2 on a material, M:

$$\mathrm{M} + \mathrm{CO_2} \rightleftharpoons \mathrm{M \cdot CO_2} \tag{1}$$

At equilibrium, $\Delta G = 0$, and $T^* = \Delta H / \Delta S$, where T^* is the turning temperature and ΔS is the entropy of reaction. Since loss of translational degrees of freedom will dominate the entropy changes associated with adsorption, we can use it as a rough estimate of ΔS. The loss of translational degrees of freedom also occurs during vaporization and is the basis of Touton's rule, which states that the heat of vaporization (in cal/mol) of nonpolar liquids is 22 times the absolute temperature (90.5T in J/mol). Using -90.5 J/mol/deg as an estimate for ΔS, and 300 K for T^*, ΔH would be only 27 kJ/mol (6.6 kcal/mol) at a CO_2 partial pressure of 1 atm. At reduced partial pressures, the optimal heat of adsorption should be corrected for the $RT \ln P$ term, and is, therefore, slightly higher. At a CO_2 partial pressure of 0.05 atm the calculated ΔH is about 35 kJ/mol (8.4 kcal/mol).

These values are similar to those for the adsorption of N_2 over zeolites and silicalite [5], and suggest that specific chemical binding is not necessary and that materials which adsorb CO_2 by relatively weak van der Waals forces might indeed be more appropriate. The adsorption of CO_2 is somewhat stronger on these zeolites; ΔH_{ads} is in the range of 30–50 kJ/mol (7–12 kcal/mol).

Thermodynamics of cooperative binding

To validate our concept, we modeled the adsorption of CO_2 in a porous solid composed of a number of individual cells, each of which can accommodate up to four CO_2 molecules. We modeled two different

situations: the first case is that of independent binding, where the CO_2 molecules do not interact, and the second case is cooperative binding, where they do interact. As initial values, we used $\Delta S = -90.5$ J/deg/mol and $\Delta H = -27$ kJ/mol. As discussed above, these values are those for a binding with minimal interaction with the substrate. In the case of independent (or non-cooperative) binding (Case 1), the ΔH value does not change with the adsorption process. However, for cooperative binding (Case 2) the value of ΔH is made progressively more negative—the average ΔH is the same in both cases.

For Case 1, the number of sites that are occupied (N_1) can be related to the number of unoccupied sites (N_0) by the binding constant (B_0) and the partial pressure (P) of the gas:

$$N_1 = PB_0N_0 \tag{2}$$

The fraction of the bound sites (B) is thus:

$$B = PB_0/(1 + PB_0) \tag{3}$$

The binding constant B_0 can be calculated from thermodynamics:

$$B_0 = \mathrm{e}^{-(\Delta H - T\Delta S)/RT} \tag{4}$$

Using different values for ΔH and ΔS, we can calculate B_0, which when plugged into Eq. (2) gives the adsorption isotherm. An example of such a simulation, with a ΔH value of -6 kcal/mol and a ΔS value of -22 cal/mol/deg is shown in Figure 2. As expected, the fraction of bound sites goes to 0 at low pressures and is essentially 100% above a pressure of 100 atm.

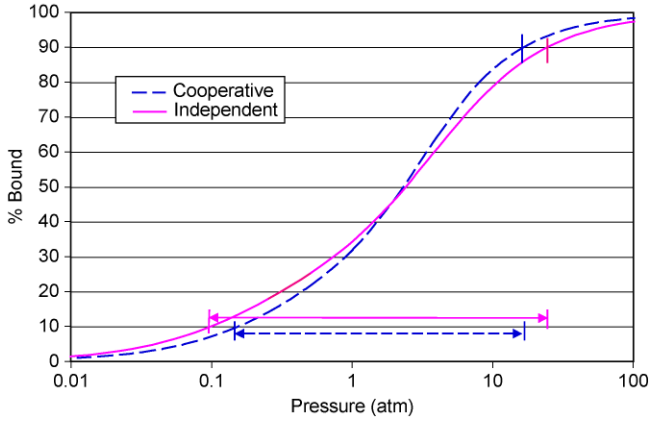

Figure 2: Adsorption isotherms for cooperative and non-cooperative binding. Non cooperative case: $\Delta H = -6$ kcal/mol. Cooperative case average: $\Delta H = -6$ kcal/mol; $\Delta\Delta H = -0.2$ kcal/mol.

Calculating the fraction of bound sites for Case 2 (cooperative binding), is a bit more involved. Here, in each cell there are four sites where a CO_2 molecule can reside. For simplicity, we assume that these four sites are degenerate. First, we have to assign the ΔH for binding to the different populations of the sites, N_i where the subscript i refers to the number of CO_2 molecules in a given cell; i can have values of 0, 1, 2, or 3. There is a population of cells with all four sites occupied, N_4, but we have stipulated that there is no further binding of CO_2 to this site. Thus, ΔH_0 refers to the heat of adsorption of CO_2 to a cell with no other CO_2 molecules in it. Likewise, ΔH_1 refers to the adsorption of the second CO_2 molecule in that cell. For the model that we developed, we kept the energy spacing between the four levels occupancy the same, in other words the $\Delta\Delta H$ was held constant. Furthermore, for a direct comparison with a non-cooperative case, we wanted to keep

ΔH_{av} the same as ΔH in the independent case. Thus,

$$\Delta H_0 = \Delta H - 2.5\Delta\Delta H \tag{5}$$

$$\Delta H_1 = \Delta H - 0.5\Delta\Delta H \tag{6}$$

$$\Delta H_2 = \Delta H + 0.5\Delta\Delta H \tag{7}$$

$$\Delta H_3 = \Delta H + 2.5\Delta\Delta H \tag{8}$$

Before proceeding with the calculation of the populations of various cells $(N_0, N_1 \ldots N_4)$ we must take care of the statistical weighting for each population. We use subscripts a, b, c, and d to label each site within the cell to help ascertain the statistical weighting factors. Since there are four ways in which one molecule can be present in a cell, the statistical factor for N_1 is 4. If we denote N_a as the cells with only position a occupied, we can generalize:

$$N_1 = 4N_a = 4N_b = 4N_c = 4N_d \tag{9}$$

Similarly, there are six ways in which two CO_2 molecules can be placed into a cell that has four positions, and so the weighting factor for N_2 is 6:

$$N_2 = 6N_{ab} = 6N_{ac} = 6N_{ad} = 6N_{bc} = 6N_{bd} = 6N_{cd} \tag{10}$$

and the weighting factors for N_3 and N_4 are, respectively, 4 and 1.

The next step in describing the cooperative effect is to incorporate the relative binding constants to provide a way of determining the total number of positions that are bound. In the first case, where one molecule is bound, we can describe it as a function of the product of the pressure of the system (P), multiplied by its initial binding constant with no other molecules around (B_0), multiplied by the initial population with no sites occupied (N_0). That value can be denoted as N_a (Eq. (11)). When we consider the adsorption of the next molecule in the cell, the population N_{ab} is equal to the population of the previous state (N_a) multiplied in the same manner by the pressure (P) times the binding constant for the second molecule. Eqs. (11–14) relate populations N_a, N_{ab}, N_{abc}, and N_{abcd} to N_0 through their respective binding constants, B_i:

$$N_a = PB_0N_0 \tag{11}$$

$$N_{ab} = PB_1N_a = P^2B_0B_1N_0 \tag{12}$$

$$N_{abc} = PB_2N_{ab} = P^3B_0B_1B_2N_0 \tag{13}$$

$$N_{abcd} = PB_3N_{abc} = P^4B_0B_1B_2B_3N_0 \tag{14}$$

As before, the values for different binding constants (B_i) can be calculated from the differences in the free energies of the states (Eq. (4) together with Eqs. (5)–(8)). By plugging in the values of B_i in Eqs. (11)–(14) and the statistical weighting factors, we can calculate the populations N_i corresponding to the cells with varying degrees of occupancy. The total number of bound sites is:

$$\text{Bound Sites} = N_1 + 2N_2 + 3N_3 + 4N_4 \tag{15}$$

and, since each cell contains four sites, the total number of sites is:

$$\text{Total Sites} = 4(N_0 + N_1 + N_2 + N_3 + N_4) \tag{16}$$

We developed an Excel worksheet that can be used interactively to generate expected isotherms as a function of changes in the ΔH and $\Delta\Delta H$ values. An example of such a simulation is also shown in Figure 2. As hypothesized, the cooperative case has a steeper adsorption isotherm. The horizontal lines show the pressure swing (P_{high}/P_{low}) that is needed in both cases for switching between 90 and 10% bound (net 80%). The pressure swing in the cooperative case is about a factor of four less for the same extent of switch.

Alternatively, if we impose the same pressure swing on the independent case, the percent change between bound and unbound would be from 82 to 16% (net 66%). In other words, a pressure swing that transports 66 molecules in the independent case, would transport 80 molecules in the cooperative case; an approximately 20% gain in efficiency.

We also varied the $\Delta\Delta H$ parameter to see its effect on the adsorption isotherm. We found that increasing its absolute value makes the curve even steeper. Also, by reducing it to zero, the resulting curve is identical with that for the independent case (Case 1). This concordance provides validation for the algorithm used in Case 2.

Potential Impact of Nanoporous Solids on PSA

A "back-of-the-envelope" estimation of the potential benefits of using the proposed nanoporous materials as compared to zeolites in a pressure swing adsorber (PSA) for the purpose of capturing CO_2 from the flue gas was also included in this task. We considered two main factors for the purpose of this analysis: capacity and thermodynamics. There are marked advantages to be realized from consideration of both factors.

Capacity

The first factor we consider is the capacity of the material for adsorbing CO_2 (q_{max}, mol CO_2/kg solid). For the moment, we assume that thermodynamic factors (heats of adsorption and cooperativity) are the same for zeolites and the copper dicarboxylates. For zeolites, literature data are available, and ZSM-5 is reported to adsorb 3 mol CO_2/kg. For the copper dicarboxylate systems, we used the information provided by Seki in the context of methane adsorption. Seki [2] reports the adsorption capacity of the biphenyl dicarboxylic acid to be 212 cm^3 of methane (STP) per gram of the salt, which translates to 9.5 mol of gas/kg solid. This is a very high value, and in a review article for *Nature*, Davis writes that the adsorption capacity of the salts synthesized by Seki "exceeds that of any other known crystalline material" [6]. The very large capacity arises from the optimal use of the framework to engineer the nanopores. In zeolites, there are many more atoms in the framework that do not contribute directly to the pore volume. Materials with smaller pores offer greater contact and, therefore, have higher heats of adsorption but they accommodate few moles of gas per unit weight. On the other hand, materials with large pores are not as effective because the binding gets too weak. According to Seki, the optimal material should be able to accommodate between four and five molecules in each pore.

Now, because the size of methane and CO_2 molecules are different, we may have to use a different dicarboxylic acid spacer in designing the optimal adsorber for our purpose. We used molecular modeling to determine the structure and pore sizes of several copper dicarboxylate systems. We also tested to see how many CO_2 molecules could be added into the lattice while reducing the total energy (i.e. exothermic binding). We used Accelrys code DMol3 for these calculations. DMol3 is a quantum mechanics-based method and is based on density functional theory in which the electron density is the fundamental quantity that determines the properties of a molecule or solid. Density functional theory does not rely on any empirical input and is generally applicable to a wide range of systems.

Results of molecular modeling showed that the Cu–Cu distance in copper oxalate is 6.7 Å, and we found that the binding of CO_2 took place above the plane and not in the pore. In the case of copper terephthalate, the Cu–Cu distance was 10.9 Å, and up to four CO_2 molecules could be added with positive binding energies to the lattice. Figure 3 shows the relaxed unit cell of copper terephthalate with four CO_2 molecules.

Thus, assuming that we can get a material to accommodate four CO_2 molecules in each pore, we can expect a capacity of around 9 mol CO_2/kg of solid. This value is three times that of zeolite ZSM-5. Thus, to a first approximation, it would require three times less material (gravimetrically) to effect the same separation with the novel materials that we will be deigning. One caveat to this statement is that tripling of the gas flow does not drastically alter the fluid dynamics. Further, the size of a PSA system is determined largely by the volumetric capacity of the adsorbent. The density of zeolites is around 2 g/cm^3, while that of the copper dicarboxylate salt is 1 g/cm^3. In other words, to achieve equivalent separation, the PSA system using the novel solids would be 50% smaller, even without considering any benefits from thermodynamic factors.

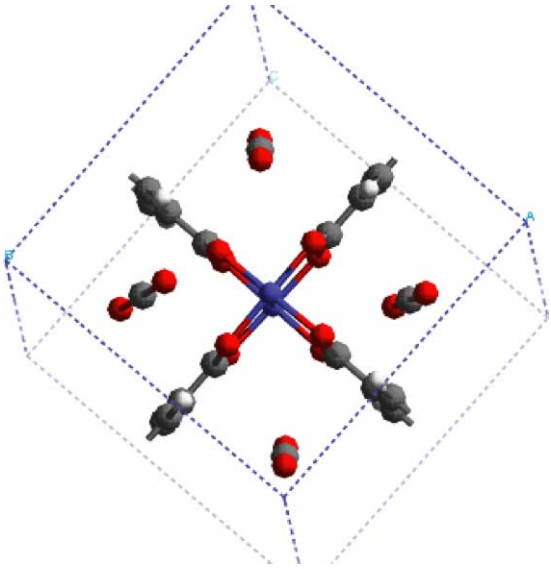

Figure 3: Relaxed unit cell of copper terephthalate showing binding of four CO_2 molecules.

Thermodynamics

The heat of adsorption (ΔH_{ads}) dictates the optimal temperature of operation of a PSA system. For zeolites, the reported ΔH_{ads} is -10 kcal/mol [5]. Invoking Trouton's rule, we can estimate the turning temperature for zeolites to be around 180 °C. The target temperature specified for this application is 40 °C, which requires the solid to have a ΔH_{ads} of -6.9 kcal/mol. If we were to operate a PSA with zeolite at 40 °C, the adsorption would be very efficient, but desorption would require pumping to very low pressures. Thus, including even a modest degree of cooperativity increases the system efficiency by 20%.

The models that simulate the PSA processes often assume Langmuir behavior and use two parameters: $\bar{q}_0$, which relates to the total capacity of the sorbent, and K, which relates to the steepness of the isotherm. These parameters are extracted by inverting the adsorption isotherm to obtain a linear equation. To make sure that the isotherms we calculated for cooperative systems can be expressed in the Langmuir form, we performed the same operation on the calculated isotherms. Since the fraction bound, B, is the moles of CO_2 bound ($\bar{q}$) divided by the maximum capacity ($\bar{q}_0$), we can rewrite Eq. (3) as:

$$\bar{q}/\bar{q}_0 = PB_0/(1 + PB_0) \tag{17}$$

Inverting Eq. (17), we get:

$$\bar{q}_0/\bar{q} = 1/PB_0 + 1 \tag{18}$$

or,

$$1/\bar{q} = (1/P)(1/\bar{q}_0 B_0) + 1/\bar{q}_0 \tag{19}$$

Thus, a plot of the inverse of the amount bound against the inverse of the pressure, the slope of which relates to the binding constant and the intercept relates to the capacity. Figure 4 shows such plots for the Case 1 and Case 2 adsorption isotherms drawn in Figure 2.

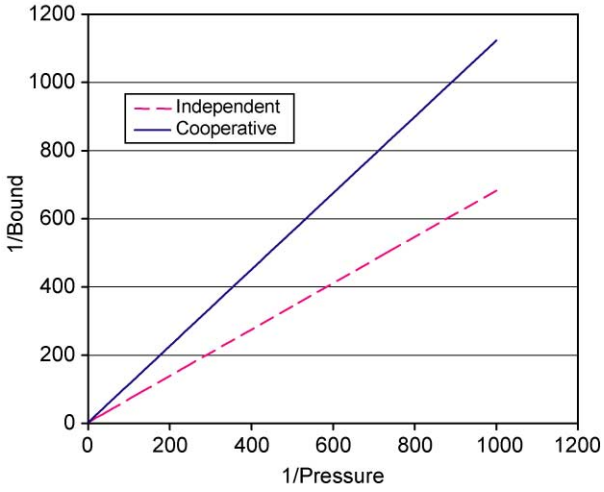

Figure 4: Reciprocal plots for isotherms in Figure 2.

The linearity for the cooperative case seen in Figure 4 verifies that these cases can also be modeled with Langmuir isotherms. Second, the near doubling in slope, which is a measure of the binding constant, is perhaps a more graphic illustration of the impact of cooperativity than could be gleaned by inspecting Figure 2.

Modeling Breakthrough of Gases

The analysis that we have so far presented relates to the fundamental properties of the adsorbent, namely capacity and heats of adsorption. However, the effectiveness with which CO_2 is adsorbed by a bed depends not only on structural characteristics but also on operating conditions. It is, therefore, important to assess the effective adsorption capacity of the solid in a given bed geometry. We developed a model to calculate the breakthrough of CO_2 through packed beds as a function of material characteristics and operating conditions. The model is general enough and includes effects of dispersion, variation of isotherms, and process conditions such as temperature, flow rate, column dimensions, adsorbent capacity, adsorbent size, and other typical parameters.

The governing equations for mass transfer in a packed bed [7,8] are:

$$-E\frac{\partial^2 c}{\partial z^2} + v\frac{\partial c}{\partial z} + \frac{\partial c}{\partial t} + \left(\frac{1-\varepsilon}{\varepsilon}\right)\frac{\partial \bar{q}}{\partial t} = 0 \tag{20}$$

$$\frac{\partial \bar{q}}{\partial t} = k(c - c^*) \tag{21}$$

$$z = 0, t > 0, c_0 v = cv - E\frac{\partial c}{\partial z} \tag{22}$$

$$z = L, t > 0, \frac{\partial c}{\partial z} = 0 \tag{23}$$

$$z > 0, t = 0, c = \bar{q} = 0 \tag{24}$$

where E is the dispersion coefficient, $c(z,t)$ is the concentration of the solute in the bulk, z is position along the bed length, v is the interstitial velocity, t is time, ε is the bed porosity not including the porosity of the particles themselves, $\bar{q}(z,t)$ is the concentration of solute on the adsorbent, k is the mass transfer coefficient (external film resistance assumed to dominate mass transfer to the particle), $c^*(z,t)$ is the bulk solute concentration that would be in equilibrium with $\bar{q}(z,t)$. It is important to note that c is the solute concentration per volume of fluid while $\bar{q}$ is the solute concentration per volume of adsorbent.

We used a Langmuir isotherm to describe the equilibrium between the solute on the adsorbent and that in the bulk fluid. As shown above, the behavior of even systems exhibiting cooperative can be adequately described in the Langmuir form:

$$\bar{q} = \bar{q}_0 \frac{Kc^*}{1 + Kc^*} \tag{25}$$

where $\bar{q}_0$ and K are curve-fit parameters. These equations may be rendered dimensionless:

$$-\frac{1}{Pe}\frac{\partial^2 u}{\partial x^2} + \frac{\partial u}{\partial x} + \frac{\partial u}{\partial \theta} + \eta \frac{\partial w}{\partial \theta} = 0 \tag{26}$$

$$\frac{\partial w}{\partial \theta} = \xi(u - u^*) \tag{27}$$

$$x = 0, \theta > 0, -\frac{1}{Pe}\frac{\partial u}{\partial z} + u = 1 \tag{28}$$

$$x = 1, \theta > 0, \frac{\partial u}{\partial x} = 0 \tag{29}$$

$$x > 0, \theta = 0, u = w = 0 \tag{30}$$

where Pe is the Peclet Number defined as:

$$Pe = Lv/E \tag{31}$$

and η and ξ are dimensionless parameters defined as:

$$\eta = \frac{1 - \varepsilon}{\varepsilon}\frac{\bar{q}_0}{c_0}, \xi = \frac{kaLc_0}{v\bar{q}_0} \tag{32}$$

and the remaining terms are defined as:

$$x = \frac{z}{L}, u = \frac{c}{c_0}, w = \frac{\bar{q}}{\bar{q}_0}, \theta = \frac{vt}{L} \tag{33}$$

The Lagmuir isotherm reduces to:

$$u^* = \frac{1}{\lambda}\frac{w}{1 - w} \tag{34}$$

where λ is defined as:

$$\lambda = Kc_0 \tag{35}$$

The above set of differential equations are solved using the Galerkin finite element method. In the case of sharp breakthrough curves, sufficient nodes must be used along with sufficiently small-time steps to ensure a stable convergence to the solution. In general, we doubled the number of nodes and halved the time step until a stable, convergent solution was obtained.

The parameters used in the above equations are either properties of the system or are estimated from the literature. The dispersion coefficient E is estimated based on Figure 4.4-4 in E.L. Cussler, *Diffusion (1985)*, whose data has been extracted and curve-fitted over a wide range of Reynold's numbers. The mass transfer coefficient k is estimated from the following (shown in Table 9.3-2 in the same book):

$$\frac{k}{v^0} = 1.17\left(\frac{\mathrm{d}v^0}{\nu}\right)^{-0.42}\left(\frac{\nu}{D}\right)^{-0.67} \tag{36}$$

where v^0 is the superficial velocity, d is the diameter of the particle, ν is the kinematic viscosity and D is the diffusion coefficient of CO_2 in air. Kinematic viscosity and diffusion coefficient were obtained from standard handbooks and adjusted for temperature and pressure.

Results

As a test case, we simulated the breakthrough of CO_2 through a cylindrical bed 5 m in diameter and 50 m in length filled with carbon by using the adsorption data from Berlier and Frere [9]. From these data, we computed the isotherm and extracted the Langmuir parameters. At this stage, we received from CCP the specific conditions of the gas flow that they wanted us to model. The concentration of CO_2 was 3.11 mol% in nitrogen and the total gas pressure was 1.28 atm. The gas was at 40 °C and the flow rate was 17,129 kmol/h. With these specified conditions, the simulation ran smoothly, and the results are shown in Figure 5. The total volumetric flow is huge, and we are not yet at a position to design a process. Besides, as yet, we do not even have any experimental values, and the objective of this exercise is simply to estimate the impact the adsorber might have on account of increased capacity and any cooperativity.

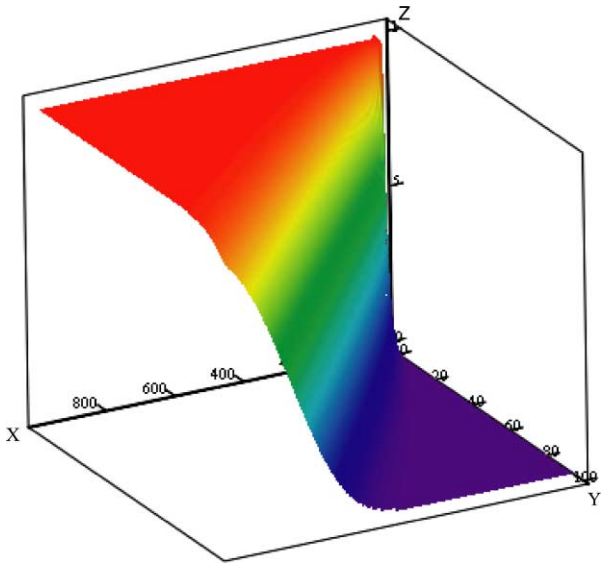

Figure 5: Simulation of breakthrough of CO_2 through activated carbon bed at 1.28 atm.

The vertical axis (Z) in Figure 5 is the concentration of CO_2 in the vapor phase as a function of time (X) and bed depth (Y) in dimensionless units. Near the head of the bed, the concentration reaches the saturation levels at short times, but deeper in the bed, the concentration rises at longer times. Furthermore, near the head of the column the break through profile is sharp, but at greater depths, the breakthrough profile is more sigmoidal. This result means that not all of the adsorbent is fully equilibrating with the gas flow.

Because the binding of CO_2 to carbon, zeolites or the nanoporous materials we are studying is weak, only a small fraction of the possible sites will be occupied at low pressures. Thus, we explored the simulations at total gas pressure 100 atm, and as expected the higher pressure improved the mass transfer between the gas and solid. The net result is that the breakthrough curve becomes very sharp. The higher equilibrium capacity combined with better mass transfer means that at high pressure we can use the bed more effectively. It also means that we can more readily compute the amounts of sorbents needed by simple equilibrium considerations. The results of transport through the carbon bed at 100 atm is shown in Figure 6. Because the concentration gradient is very sharp, the simulation introduces some artificial oscillations. Nevertheless, we can see that the breakthrough is sharp at all depths, which means that the adsorbent bed is being used effectively. We recognize that the pressurization of the entire flue gas is likely to require considerable energy, and therefore we may need to find materials with heats of adsorption near 8.4 kcal/mol instead of the 6.0 kcal/mol that we used in these simulations.

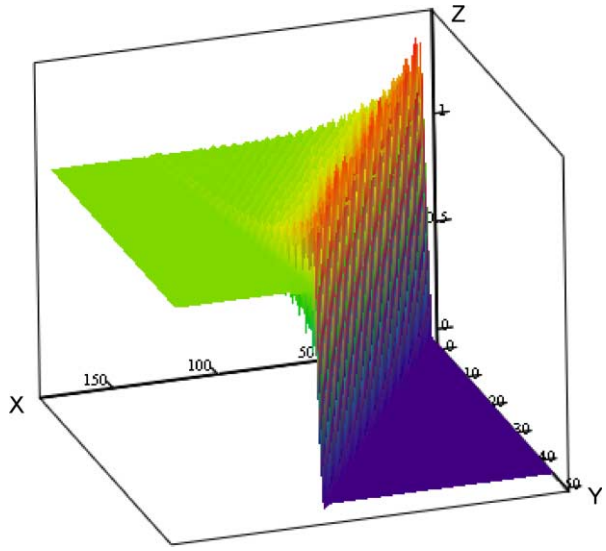

Figure 6: Simulation of breakthrough of CO_2 through activated carbon bed at 100 atm.

We also simulated the breakthrough of CO_2 through cylindrical beds (1.8 m diameter × 10 m long) of activated carbon and copper terephthalate. The bed dimensions were chosen to make the breakthrough time for the carbon case around 3 min, which is typical of a PSA cycle. For the activated carbon, we used the Langmuir parameters that we had extracted from the literature [9]. The adsorption capacity was 3.6×10^{-3} g mol/cm^3 and the K parameter was 0.406 atm^{-1}. Since there are no experimental values for these parameters for copper terephthalate we had to estimate them. For the capacity factor, our estimation was based on the expectation that similar to case of methane, four CO_2 molecules could be accommodated in each cell. This value gives a capacity factor of 9.5 g mol/kg. Because of its porous structure, copper terephthalate is likely to be less dense than other oxide structures like zeolites (2.0 g/cm^3). For our simulation we used 1.0 g/cm^3 as the density, and hence a Langmuir capacity factor of 9.5×10^{-3} g mol/cm^3. As for the K factor,

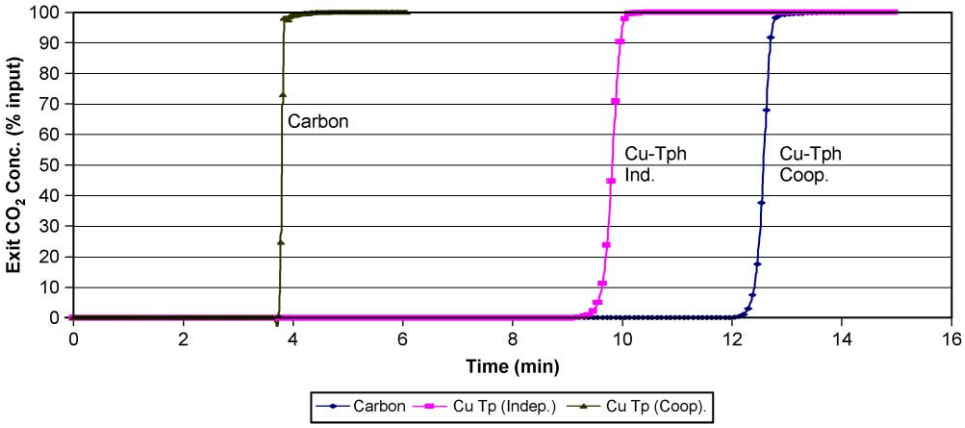

Figure 7: Breakthrough of CO_2 through a packed bed (10 × 1.8 m^2) of carbon and copper terephthalate (independent and cooperative binding).

we investigated two cases. The first one being the same value as for carbon, and then we used a K factor that was twice as large to mimic cooperative binding. The results are shown in Figure 7.

The breakthrough times for copper terephthalate (independent or cooperative) are substantially longer. This result means that considerably smaller beds of this material could be used to effect equivalent separation. If we keep the diameter fixed at 1.8 m, the appropriate bed length would be 3.2 m, or about a third that for carbon if copper terephthalate displayed no cooperativity. The bed length could be further reduced to 2.5 m, if we observed a modest degree of cooperative binding. These size reductions should translate into substantial reductions in capital and operating expenditures.

CONCLUSIONS

We have shown that for optimal capture of CO_2 in a PSA system operating around ambient temperature, it is desirable that the heat of adsorption be only around 27 kJ/mol (6.6 kcal/mol), or around 35 kJ/mol (8.4 kcal/mol) if the CO_2 concentration is only 5%. Further, nanoporous solids, which can have very large adsorption capacities offer the benefit of reducing the bed size and thereby the mechanical work required for pressurization and depressurization. Further reduction in bed volume can be realized with systems that display cooperative behavior.

NOMENCLATURE

$\bar{q}$	concentration of solute on the adsorbent
θ	dimensionless time
B	binding constant
c	solute concentration in the vapor phase
D	diffusion coefficient in air
d	particle diameter
E	dispersion coefficient
k	mass transfer coefficient
N	number of cells (or sites when cells can have only unit occupancy)
P	pressure
Pe	Peclet number
PSA	pressure swing adsorption
T	absolute temperature
t	time
u	dimensionless solute concentration in vapor phase
v	interstitial velocity
v^0	superficial velocity
w	dimensionless solute concentration in solid phase
x	dimensionless length
ε	bed porosity
ΔG	change in free energy
ΔH	change in enthalpy
ΔS	change in entropy
η	dimensionless parameter
ν	kinematic viscosity
ξ	dimensionless parameter

ACKNOWLEDGEMENTS

We acknowledge many fruitful discussions with Drs Piergiorgio Zappelli and Daniel Chinn during the course of our project that helped clarify our concepts.

REFERENCES

1. K. Seki et al., *US Patent No. 5,998,647*, Dec. 1999.
2. K. Seki, *Chem. Commun.* (2001) 1496–1497.
3. K. Seki, W. Mori, *J. Phys. Chem. B* **106** (2002) 1380.
4. A.L. Lehninger, *Biochemistry*, second ed., Woth Publishers, New York, 1975, p. 236.
5. J.A. Dunne, et al., *Langmuir* **12** (1996) 5896.
6. M.E. Davis, *Nature* **47** (2002) 813–821.
7. R.T. Yang, *Gas Separation by Adsorption Processes*, Butterworth, Boston, 1987.
8. E.L. Cussler, *Diffusion: Mass Transfer in Fluid Systems*, second ed., Cambridge University Press, New York, 1997.
9. K. Berlier, M. Frere, *J. Chem. Engng. Data* **41** (1996) 1144.